Intensity Modulated Radiotherapy Target Volume Definition by Means of Wavelet Segmentation

Tsair-Fwu Lee[1], Pei-Ju Chao[2], Fu-Min Fang[1], Eng-Yen Huang[1], and Ying-Chen Chang[2]

[1] Chang Gung Memorial Hospital-Kaohsiung, 83342, Taiwan, ROC
[2] Kaohsiung Yuan's General Hospital, Kaohsiung, 800, Taiwan, ROC
alf@adm.cgmh.org.tw, pjchao@bit.kuas.edu.tw

Abstract. This study aimed to develop an advance precision three-dimensional (3-D) image segmentation algorithm to enhance the blurred edges clearly and then introduce the result onto the intensity modulated radiotherapy (IMRT) for tumor target volume definition. This will achieve what physicians usually demand that tumor doses escalation characteristics of IMRT. A proposed algorithm flowchart designed for this precision 3-D treatment targeting was introduced in this paper. Different medical images were used to test the validity of the proposed method. The 3-D wavelet based targeting preprocessing segmentation allows physicians to improve the traditional treatments or IMRT much more accurately and effectively. This will play an important role in image-guided radiotherapy (IGRT) and many other medical applications in the future.

Keywords: intensity modulated radiotherapy, target volume, wavelet, segmentation.

1 Introduction

Three-dimensional (3-D) conformal therapy has been used in most cancer patients receiving radiotherapy. The role of intensity modulated radiotherapy (IMRT) is well established due to its tumor doses escalation characteristics. The goal is to deliver as much radiation as possible to a tumor while sparing nearby normal tissue—especially critical, but radiation-sensitive organs such as the spinal cord or rectum [1-4]. Physicians need 3-D renderings to help them make diagnoses, conduct surgery, and perform radiation therapy which two-dimensional (2-D) images usually cannot offer. However, without precision segmentation these 3-D renderings could lead to misleading results. The aim of this study is to provide a precision 3-D segmentation method to achieve what physicians demanded. They will also become the preprocessing reference data to intensity modulated radiotherapy systems.

Since conventional medical images of computed tomography (CT) or magnetic resonance of imaging (MRI) although appeared to be 3-D images, they are all composed by slice-based 3-D image datasets. One effective way to obtain precision 3-D segmentation reconstruction rendering is to process the sliced data with high precision first [5, 6]. In this study, the proposed algorithm is to apply the wavelet segmentation

B. Gabrys, R.J. Howlett, and L.C. Jain (Eds.): KES 2006, Part II, LNAI 4252, pp. 1 – 10, 2006.

approaches in a maximize entropy sense. This allows us to utilize all available information to achieve the most robust segmentation results for 3-D image reconstruction. We then apply the segmentation method to medical images including two CT scan image and one MRI image to test the validity of our method and to compare the precision with a conventional segmentation approach. We aim to show the 3-D segmentation method is superior in precision with only a reasonable amount of computing time. From the mathematical viewpoint, since images are 2-D arrays of intensity values with locally varying statistics, different combinations of abrupt features like edges and contrasting homogeneous regions are better to process with wavelet-based transformations which is known to have the advantage of multi-resolutions. We shall see this indeed was feasible and the results are quite satisfactory.

2 Wavelet Segmentations

In recent years, wavelet theory is widely used in various signal-processing problems. Its great flexibility makes it the most desired signal processing technique in many applications. In this section we introduced the idea of multiresolution first and then developed the Discrete Wavelet Transform (DWT). We then extended the DWT into two dimensions and derived a two-dimensional Discrete Wavelet Transform (2-D DWT) by separate algorithms. Finally, we should develop the wavelet edge detector from the 2-D DWT.

The Wavelet method is known to be one of the best gradient segmentation methods due to its multi-scale and multi-resolution capabilities. Assume $S_{2^j}[\ ]$ and $D_{2^j}[\ ]$ as the low pass signal and the high pass signal of $f(x)$ at resolution 2^j respectively, and $S_{2^j}[n]=\langle f(u),\phi_{2^j}(u-2^{-j}n)\rangle$ is the projection coefficient of $f(x)$ on V_j, $D_{2^j}[n]=\langle f(u),\varphi_{2^j}(u-2^{-j}n)\rangle$ is the projection coefficient of $f(x)$ on O_j .We can define an orthogonal complement subspace of V_j as O_j, in space V_{j+1}. In other words, $O_j \perp V_j$ and $O_j \oplus V_j = V_{j+1}$, where V_j is the expansion of $\phi(x)$ by basis $\sqrt{2^{-j}}\phi_{2^j}(x-2^{-j}n)_{n\in Z}$, O_j is the expansion of $\varphi(x)$ by basis $\sqrt{2^{-j}}\varphi_{2^j}(x-2^{-j}n)_{n\in Z}$, $\oplus$ denotes the union of space (like the union of sets) and $\perp$ denotes two sets are orthogonal. The scaling function $\phi(x)$ and wavelet function have the orthogonal properties as shown in [7-9]. By the properties of multi-resolutions, a signal can always be decomposed into higher resolutions until a desired result is reached. This can be interpreted by tree architectures known as the Pyramid architecture [9]. Hence we may create a 2-D filter for edge detection by replacing the traditional 2-D wavelet functions with a 2-D discrete periodic wavelet transform (2-D DPWT) [8]. The 2-D DPWT can be written in the matrix form as follows: $[SS_{j+1}]_{N_1\times N_1}=W_{LL}\otimes[SS_j]_{N_2\times N_2}$, $[SD_{j+1}]_{N_1\times N_1}=W_{LH}\otimes[SS_j]_{N_2\times N_2}$, $[DS_{j+1}]_{N_1\times N_1}=W_{HL}\otimes[SS_j]_{N_2\times N_2}$, and $[DD_{j+1}]_{N_1\times N_1}=W_{HH}\otimes[SS_j]_{N_2\times N_2}$. Where $N_1=2^{|j+1|}$, $N_2=2^{|j|}$, W_{LL}, W_{LH}, W_{HL} and W_{HH} are the four subband filters; $\otimes$ denoted a convolution operation; $S_{2^j}[\ ]$ is the low pass signal, or the approximated signal; $D_{2^j}[\ ]$ is the high pass signal, or the detailed

signal of $f(x)$ at resolution 2^j respectively. For 2-D images, they are in the form of $[SS_{j+1}]_{N_1 \times N_1}$ which come from $[SS_j]_{N_2 \times N_2}$ convoluted with the corresponding subband filter W_{LL}, where $[SS_j]_{N_2 \times N_2}$ is a matrix form the expanded image. The definition of the four subband filters' operators of 2-D DPWT are [7-9]: $W_{LL} = [h(i) \cdot h(j)]_{i,j \in Z}$, $W_{LH} = [(-1)^{3-j} h(i) \cdot h(3-j)]_{i,j \in Z}$, $W_{HL} = [(-1)^{3-j} h(3-i) \cdot h(j)]_{i,j \in Z}$, and $W_{HH} = [(-1)^{i+j} h(3-i) \cdot h(3-j)]_{i,j \in Z}$. Where $h(i) = < \phi_{2^{-1}}(u) \cdot \phi(u-i) >$. Clearly, since the coefficients of the filter have length *d*, the operator of 2-D DPWT formed a $d \times d$ matrix. We now use the coefficients of the four filters given by the above equations to generate a wavelet edge detector.

Let $f_h(i, j)$ be the horizontal high-pass filter function and $f_v(i, j)$ be the vertical high-pass filter function obtained from the four operators of 2-D DPWT

$$f_h(i, j) = W_{LL}(i, j) \otimes W_{LH}(i, j) \tag{1}$$

$$f_v(i, j) = W_{LL}(i, j) \otimes W_{HL}(i, j) \tag{2}$$

We now apply the different length coefficients of Daubechies wavelet transform to generate multi-scale masks for images segmentation in different scales [7-9].

Next, let the original image pass through these masks to produce a series of multi-scale images with different gradient strengths. In order to avoid distortions caused by noise and to define exact edge points, an edge thinning technique is then used to make effective determination of the images. This can be done by observe a line through each pixel along its gradient direction first. If the pixel is local maximum along that line, we retain the pixel, or else we suppress it. We shall complete the 2-D image of each slice and then join the edges to form a surface. The advantage of processing 2-D images this way is obvious. Both storage and computation time were much less and parallel processing can be easily done.

3 Flowchart of the Proposed Method

The goal of any precision image segmentation is to partition an image into disjoint regions of desired objects as accurate as possible. The multi-resolution nature of a wavelet operator allows us to detect edges at different scales. In the wavelet edge detection algorithms, the transformation uses DPWT and the filter searches for local maximal in the wavelet domain. Many earlier researches proved that the wavelet edge detector can detect very complicated edges [10-13]. Therefore if we improve the wavelet transform further in the maximal entropy manner, we expect better results beyond any segmentation method are capable alone. The following descriptions are our precision 3-D treatment targeting reconstruction renderings applied to medical images [14]. The treatment targeting rendering algorithm which utilized the wavelet segmentation approaches is shown in Fig. 1. Figure 2 is a slice of the CT images of human chest. We then compared the quality of the segmentation results with a traditional method named region growing to show how the proposed algorithm did better in precision targeting. The processing steps are:

1) 2-D CT slices of human chests are very common in medical examinations, but they usually differ greatly in illumination contrasts. Therefore normalization is needed. CT images of 512*512*16 bits in the DICOM (Digital Image and Communication in Medicine) format bits are now normalized between 0 and 1.
2) Next we make a Region-of-Interest (ROI) selection. The ROI shall be our *a priori* knowledge in the segmentation algorithm. It defined the object we desire to inspect, whereas the rest of the image is treated as backgrounds. We then select a mask roughly covers the ROI. In this case the right lung is our desired object in this experiment, ROI and a mask of an initial shape covers the right lung is formed. At the same time the image were send through a bank of homomorphic filters and lower-upper-middle filters to smooth and sharpen the object that we want to segment.
3) The ROI partitioned image is now cut out. It shall be processed separately to increase efficiency.
4) We process the partitioned image via wavelet edge detection and region-growing segmentation [15] separately for comparison.
5) The wavelet segmented images is now selected for comparing pixel-by-pixel with their *a posteriori* probability to find the true edge.

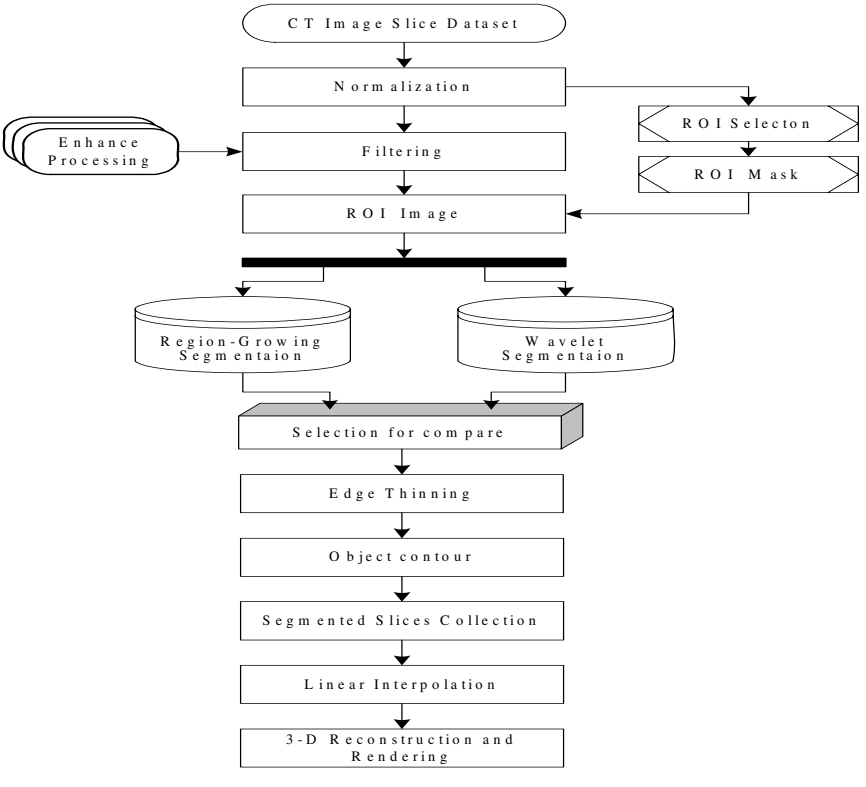

Fig. 1. The flowchart of the 3-D treatment target reconstruction rendering

6) Edge thinning comes next. Since our method pertain pixels with the same or similar strength, it may result in thick edges. But our objective is to segment the target precisely. Hence nearest neighborhood algorithm is next applied to create a thinning process to obtain the contour of the desired object. The contour is then inserted back into the original image.
7) As the contour is insert back into the original image, there will be missing areas plus contrast differences. Dilation algorithm and Erosion algorithm were then applied to fill the gaps and to obtain the object respectively.
8) Slices with segmented objects are now collected for 3-D reconstruction.
9) We process the segmented slices with linear interpolations to form a 3-D rendering of the object.
10) Tiling algorithm which patches the stacking contours is now applied to form surfaces [13, 16]. The 3-D reconstruction is now completed and the target shows out for treatment procedure.

4 Experiment Results

In the first experiment, original slices of a human chest from CT scan are used, with one of the slice enlarged in Fig. 2 (a). We performed the 2-D segmentation first slice by slice. Since we aim to extract the right lung for feature extraction it becomes our natural ROI selected by using the cursor which is shown in the Fig. 2 (b). Fig. 2 (c) shown the region-growing contour; Fig. 2 (d) illuminated the wavelet contour; Figs. 3 (a) (b) showed the segmentation results of Figs. 2 (b), (c) respectively. On close inspection of these figures, shortcoming of lack of smoothness from both our wavelet segmentation method and that from the traditional region-growing method were obvious, but seemed to be harmless. However, as 3-D renderings were formed, they create errors, and shall not be tolerated if precision renderings were sought. Fig. 3 (c) shows the 3-D rendering from the region-growing segmentation. Fig. 3 (d) shows the 3-D rendering from the wavelet segmentation. If we look at them closely, we found that the 3-D renderings by the region-growing segmentation, seemed acceptable, but it has problems that at times a single slice will be very different from the others at some particular point due to noise and/or other disturbances, which makes the corresponding 3-D renderings appeared with wrinkles. Clearly human lungs should be continuous and smooth in all directions always; hence we conclude that the region-growing method is unable to reconstruct the object precisely. On the other hand, our wavelet segmentation with maximum entropy approaches creates a 3-D reconstruction rendering much more correctly. Hence the proposed method is superior to many current methods.

The next experiment is processing a CT scan of a female patient with a pituitary tumor in her brain. The pituitary gland is about the size of a pea at the center of brain just at the back of the human nose. It makes hormones that affect growths and functions of other glands. Tumors that make infectious hormones are known as functioning tumors, which are most deadly. The choice of treatment on this kind of tumor uniquely depends on the position and orientation of the tumor. With a target so small and so vital, only position of the tumor pin down with the highest precision, treatments can then be effective, and ordinary brain cells can be spared the doses.

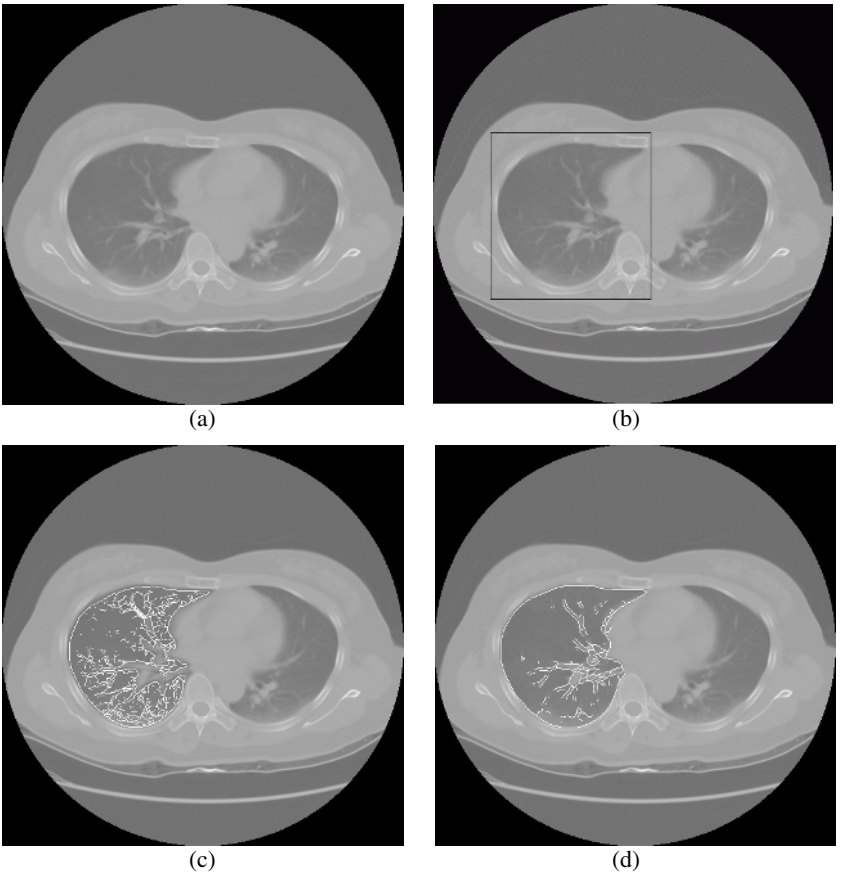

Fig. 2. (a) A selected original image. (b) A selected ROI in the original image. (c) Segmented contour by the region-growing method. (d) Segmented contour by the wavelet method (white line).

The original slices are shown in the Fig. 3 (a) where the tumor can hardly be seen visually. We first segmented it out with great precisions, and then insert it back into the original images with a strong contrast as shown in Fig. 3 (b). The tumor can now be clearly inspected. Comparison of Fig. 3 (a) and 3 (b) clearly demonstrated the advantage of our segmentation; it provided an outstanding positioning of the tumor which has not been achieved by other 3-D renderings so previously.

3-D treatment targeting segmentation renderings of the pituitary tumor are next reconstructed. Its various angles are shown in Fig. 5 (a-h). We shall test the accuracy of localization of our method by using coloring and a so-called transparency technique, we shall find not only we can identify the problem area precisely, but also their relative positions to other critical organs are all clearly shown. The size and shape of the tumor, its orientation with the brain, and the position relative to the head are all now

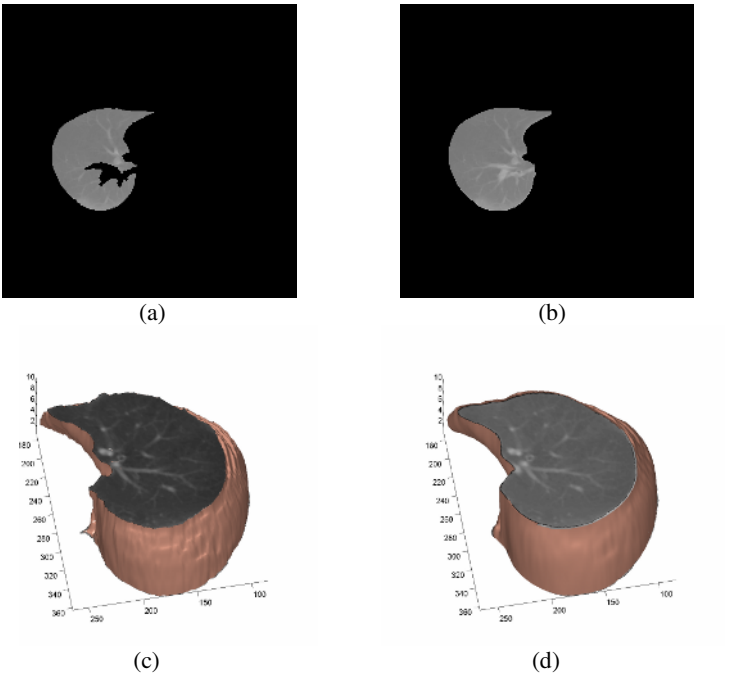

Fig. 3. (a) Segmented result of the region-growing method. (b) Segmented result of the wavelet method. (c) 3-D target reconstruction rendering by the region-growing method. (d) 3-D target reconstruction rendering by wavelet method.

clearly seen. These 3-D treatment targeting segmentation renderings can be rotated to any angle and with different colors for inspections. Transparency effect is now introduced in the last line. They shall be most useful for intensity modulated radiotherapies.

In the next example, we demonstrate further how colors were used in our 3-D wavelet based segmentation renderings to enhance the important parts. Slices of a human head from a MRI modality are used in this experiment. Our 3-D rendering method allows us to display the skull of the patient, or his brain, or both in all angles. We obtain a 3-D rendering of the skull quickly by noticing that the skull bone has a special feature of being dense and uniform, which clearly stands out in grey levels in each 2-D slice, segmentations hence becomes easy. The original slices of a human head from a MRI modality are reconstructed in Fig. 6(a). The result 3-D renderings of different angels of the skull are shown in Fig. 6(b).

To obtain a 3-D rendering of the brain, the skull rendering successfully constructed is now removed from the original image as shown in Fig. 6 (c). Finally, 3-D reconstruction of the brain in a partial skull is shown in Fig. 6 (d) with different colors to emphasize their relative positions. The superiority of our algorithm is now demonstrated by real medical images in terms of precision and efficiency.

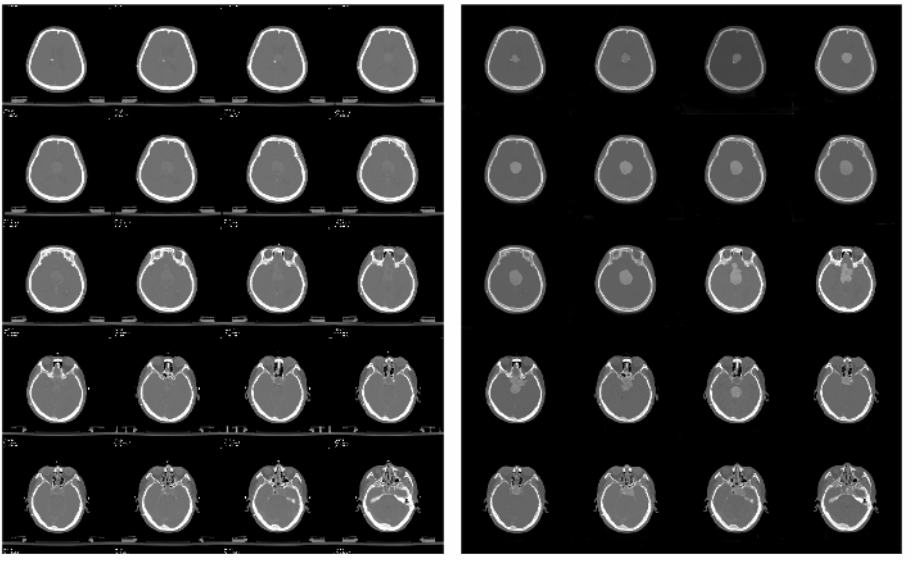

(a) (b)

Fig. 4. (a) The original slices from a CT modality. (b) The enhanced tumor image inserted back into the original image slices.

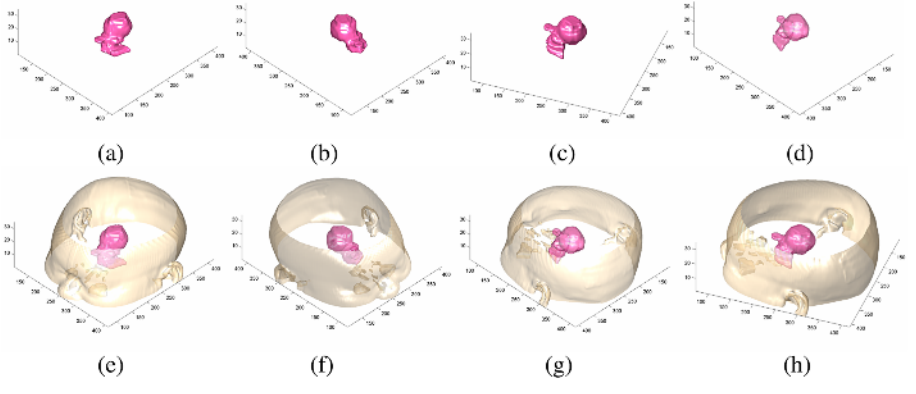

(a) (b) (c) (d)

(e) (f) (g) (h)

Fig. 5. 3-D treatment target reconstruction renderings of the tumor with transparent effect

We have successfully completed 3-D medical renderings with great precisions. These images although stacked by 2-D images, but resulting from processing by a maximum entropy method, hence mathematically optimal in statistical sense. We further prove our method is indeed practical by processing real medical images.

On all examples of medical images we processed, not only desired precision had been achieved, we were also able to create rotation of the objects to obtain its 3-D

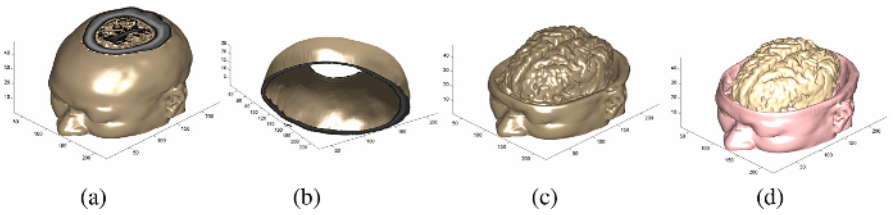

Fig. 6. (a) 3-D reconstruction of the original slices. (b) 3-D reconstruction of the skull. (c) 3-D reconstruction of the brain in an imaginary opened head. (d) An imaginary opened head in different colors.

images of different angles. We were also capable to show layers and features, organs and bones. We could emphasize the interested areas by adding various colors to them on purposes, or we could diminish the less important parts by applying the transparent effect. The 3-D renderings we created will allow physicians to conduct surgery or treatment much more accurately and effectively.

We have presented our results to seven doctors of the Department of Radiation Oncology. They examined them closely and all agreed they were superior than any rendering they have seen and encourage this line of research should proceed further as soon as possible.

Although our rendering method is more advance in many ways, but it still far from direct medical applications. The processing required only an ordinary PC but the processing time is considerable. This shortcoming makes it inapplicable medically for places like the emergency room where immediate results are required.

Applying our method for IMRT treatment for tumors has not been tested also. Our images no doubt shall be a great help for the physicians, but medical decisions and responsibilities lies on the shoulder of them. Whether they can totally rely on our images can be only evaluated after years of practical use.

5 Conclusions

For medical renderings, precision is our primary concern; we choose the wavelet method for its great multi-scale and multi-resolution characteristic to process 2-D slices in sequence. We further improve the wavelet method by introducing the maximum entropy sense then ensured improved accuracies. Linear interpolation was then used to form 3-D renderings, also proved to be effective and accurate. Many images of interest that physicians unable to visualize are now clearly identified, locations pinned down exactly, and relative orientations are now well understood. These are all vital for medical treatments. The preprocessing treatment targeting segmentation algorithm we developed can be extended to IMRT or image-guided radiotherapy (IGRT) easily. Features are now clearly identified, locations and size pinned down exactly, and relative orientations are now well understood. These are all definitely required for IMRT and IGRT treatments. We believe our precise 3-D treatment targeting segmentation method shall play an important role in future medical application.

References

1. Ezzell GA, Galvin JM, Low D, et al.: Guidance document on delivery, treatment planning, and clinical implementation of IMRT, Report of the IMRT Subcommittee of the AAPM Radiation Therapy Committee. Med Phys 2003; 30:2089-2115.
2. Intensity Modulated Radiation Therapy Collaborative Working Group (IMRTCWG). Intensity modulated radiotherapy: Current status and issues of interest. International Journal Radiation Oncology Biology Phys 2001; 51:880-914.
3. LoSasso T, Chui CS, and Ling CC: Comprehensive quality assurance for the delivery of intensity modulated radiotherapy with a multileaf collimator used in the dynamic mode. Med Phys 2001; 28:2209-2219.
4. Low DA: Quality assurance of intensity-modulated radiotherapy. Semin Radiat Oncol 2002; 12:219-228.
5. Chakraborty A: Feature and Module Integration for Image Segmentation. PhD thesis, Yale University, 1996; 89-185.
6. Gabriele Lohmann: Volumetric Image Analysis. Wiley & Teubner, 1998; 34-128.
7. Ku CT, Hung KC and Liag MC: Wavelet Operators for Multi-scale Edge and Corner Detection. Master thesis, Department of Electrical Engineering, I-Shou University, Taiwan, 1998; 4-65.
8. Leu YS, Chou CJ: Wavelet Edge Detection on Region-based Image Segmentation. Master thesis, Department of Computer & Communication Engineering, National Kaohsiung First University of Science and Technology, Taiwan, 2000; 8-27
9. Mallat SG: Multifrequency Channel Decompositions of Images and Wavelet Models. IEEE Transactions on Acoustics. Speech and Signal Processing, December 1989; 37. 12-17.
10. Canny JF: A Computational approach to edge-detection. IEEE Transactions on Pattern Analysis and Machine Intelligence, 1986; 8:679-698.
11. Gonzalez RC, Woods RE: Digital Image Processing. Prentice Hall, 2nd ed. Edition, 2002; 349-405.
12. Kitchen L, and Rosenfeld A: Edge Evaluation Using Local Edge Coherence. IEEE Transactions on Systems, Man, and Cybernetics. 1981; SMC-11. 9, 597-605.
13. Russ JC: The Image Processing Handbook, Third ed. CRC Press & IEEE Press, 1999; 23-138.
14. Tsair-Fwu Lee, Ming-Yuan Cho: “Precise Segmentation Rendering for Medical Images Based on Maximum Entropy Processing”, Lecture Notes in Computer Science, vol.3683, Springer-Verlag, 2005, pp.366-373.
15. Rafael C. Gonzalez, Richard E. Woods. Digital Image Processing. Prentice Hall, 2nd ed. Edition, 2002. pp.612-617.
16. John C. Russ. The Image Processing Handbook, Third ed. CRC Press & IEEE Press, 1999.